

Latency and Information Freshness in Multipath Communications for Virtual Reality

Federico Chiariotti, Beatriz Soret, Petar Popovski

Department of Electronic Systems, Aalborg University, Denmark

Email: {fchi, bsa, petarp}@es.aau.dk

Abstract

Wireless Virtual Reality (VR) and Augmented Reality (AR) will contribute to people increasingly working and socializing remotely. However, the VR/AR experience is very susceptible to various delays and timing discrepancies, which can lead to motion sickness and discomfort. This paper models and exploits the existence of multiple paths and redundancy to improve the timing performance of wireless VR communications. We consider Multiple Description Coding (MDC), a scheme where the video stream is encoded in \mathcal{Q} streams ($\mathcal{Q} = 2$ in this paper) known as descriptors and delivered independently over multiple paths. We also consider an alternating scheme, that simply switches between the paths. We analyze the full distribution of two relevant metrics: the packet delay and the Peak Age of Information (PAoI), which measures the freshness of the information at the receiver. The results show interesting trade-offs between picture quality, frame rate, and latency: full duplication results in fewer lost frames, but a higher latency than schemes with less redundancy. Even the simple alternating scheme can outperform duplication in terms of PAoI, but MDC can exploit the independent decodability of the descriptors to deliver a basic version of the frames faster, while still getting the full-quality frames with a slightly higher delay.

Index Terms

Virtual Reality, Multiple Description Coding, video transmission, multipath, packet delay, Age of Information

I. INTRODUCTION

Over the past decade, Virtual Reality (VR) and Augmented Reality (AR) have exited the realm of science fiction and become an increasingly commonplace reality in a variety of fields, from

education [1] and medicine [2] to tourism and industry [3]. The worldwide COVID-19 pandemic has only accelerated the development of these technologies [4], as the need for social distancing has moved several aspects of work and personal life online. VR is also crucial to the *digital twin* concept, which enables remote inspection and operation of cyber-physical systems, and for human-in-the-loop control, in which parts of a manufacturing system are automated, while other parts are controlled directly by a human operator [5], [6]. In these scenarios, the timeliness of the operation is crucial, as delays can have a significant impact on the performance and even safety of the machinery. Moreover, the necessity of communication cables severely limits the mobility of both the operators and the autonomous robots.

Computational offloading can enable smooth operation on smaller devices or with mobile nodes [7], freeing AR and VR users from being tied to desktop-level computing power through direct wires which can impede movement and limit immersiveness. However, these applications can suffer from significant timeliness-related issues on wireless networks [8]: as the sense of presence and immersion is critical, and the size of each omnidirectional frame can be huge, this puts a strain on the notoriously volatile wireless links, with a high risk of congestion and sudden delay increases, which are perceived by the user as an annoying loss of smoothness in the VR experience. Adaptive video content can reduce delay by compressing the video, trading video quality for a smaller, more predictable delay [9], but the unpredictability of the wireless propagation environment can make this task very complex.

In this context, there are two metrics that can be used to evaluate the timeliness of the communication: the first, and most traditional, is the latency of the transmission, i.e., the time between when a frame is generated at the source and when it is delivered to the receiver and displayed to the user, while the second is the Age of Information (AoI). AoI is a metric that has attracted a significant interest in the research community since its inception in the early 2010s [10], as it can better represent the delay perceived by users in real-time applications. The age does not just measure the time between when a frame is generated and when it is delivered, but keeps increasing until the next frame has been delivered. As the name suggests, the AoI is the *age* of the frame that is currently on the VR display. Intuitively, AoI is more useful for control tasks, as the age of the information shown to the user will affect both the smoothness of the VR experience and the control performance: if the user makes a command, it will be based on old information, and the older the scene that the user can see, the less immediate that command will get. In particular, we consider the Peak Age of Information (PAoI), which

measures the age right before the next frame arrives, which is a good proxy for the worst-case timing discrepancy of a virtual reaction.

In this work, we consider a theoretical model of multipath VR transmission, deriving the complete distribution of the latency and PAoI analytically with four different transmission schemes. In particular, we consider both schemes that try to reduce the load on the multipath connection by splitting the traffic between the two paths and a scheme that replicates the frames on both paths to protect them from errors and delays of the individual paths. Multiple Description Coding (MDC) [11] is a scheme that can strike a balance between smoothness and quality, as it encodes the frame into multiple *descriptors*, each of which can then be delivered independently. Each descriptor can be decoded individually, resulting in a lower-quality representation, but larger numbers of descriptors can be combined to recover higher-quality representations if they are delivered on time. We draw some considerations on the performance of each scheme, finding interesting results in the trade-off between reliability (i.e., delivering as many frames as possible in error-prone scenarios), frame rate and quality, and latency or age.

The rest of the paper is organized as follows: Sec. II presents an overview of the related work on multipath multimedia communications, queuing models and AoI. Our overall system model is described in Sec. III, and the analyses for the alternating and coded systems are described in Sec. IV and Sec. V, respectively. Sec. VI then presents our simulation settings and results, and Sec. VII concludes the paper and presents some avenues of future work.

II. RELATED WORK

A. *Multipath multimedia communications*

Multipath communications can be exploited for very different applications and purposes, such as increasing the network capacity [12], increasing the reliability [13], or reducing the latency [14]. Path diversity is often used as a means to apply other redundancy schemes, such as error control coding [15]. In the case of multimedia content in real time, the use of multiple paths to overcome possible failures and blockages on any single link has been the subject of intense investigation over the past few years. For AR/VR, the higher bitrate required to transmit 360° frames can exacerbate these issues, making the benefits of multipath delivery even more evident: a higher capacity and resilience to failures or capacity drops on any single path can significantly improve the Quality of Experience (QoE) and the smoothness of remote control operations.

The Internet of Things (IoT) has seen a significant expansion in the past decade, and previously impossible video sensor applications are now commonplace: in this case, real-time operation can be required to monitor a process or an area remotely, or to control a robot's activity. In this field, energy-efficiency is a significant concern [16], and communication strategies need to take it into account: a recent survey on multipath routing in this context [17] describes several techniques that have been proposed by the research community. In this case, video quality is generally low, and the most pressing concern is routing rather than bitrate adaptation. Interestingly, the same type of concepts can also apply to VR services in heterogeneous 5G networks [18]: latency and energy-efficiency are critical metrics in small cell networks.

There has also been significant activity on the transport layer to enable end-to-end multipath communications. As the bottlenecks in the paths might not be directly observable, this is a significantly more complex problem, which intersects congestion control research and highlights some of the issues of the currently used transport protocols. The Multipath TCP (MPTCP) standard [19] was developed as an extension of TCP to multipath connections, enabling faster and more reliable delivery, but it has been shown to be unsuitable for real-time media. While early studies [20] had promising outcomes, MPTCP fell prey to the same basic issues that standard TCP has with real-time traffic [21]: namely, the potentially long delays caused by the congestion control and retransmission mechanisms if the capacity drops. Furthermore, scheduling packets over the available paths is another problem specific to multipath transmission [22], which can compound with the congestion issues and interact with congestion control in non-obvious ways [23]. As it is the most common protocol, however, MPTCP is used in a number of VR solutions [24], which devise application-level schemes to work around its issues.

In order to overcome the limitations inherent in MPTCP, there is active research on multipath versions of other protocols such as the Real-time Transport Protocol (RTP) [25] and the Stream Control Transmission Protocol (SCTP) [26], but the lack of widespread adoption makes these protocols less likely candidates for future adoption. More recently, other solutions relying on entirely new protocols have been developed: one example is the Multipath Multimedia Transport Protocol (MPMTP) [27], which uses Raptor codes to recover from packet losses without retransmissions. The more recent Latency-controlled End-to-End Aggregation Protocol (LEAP) protocol [14] also uses coding, working on blocks with adaptable size and providing reliable latency guarantees. For a more comprehensive study of multipath transport layer solutions, we refer the reader to [28]. In most of these applications, the basic trade-off is between meeting

the application’s latency, throughput, and reliability requirements and reducing the impact on other flows, as using resources on multiple paths is a greedy option that should be limited to necessary uses.

B. Queuing models

Our system model is based on a fork-join queue [29], where incoming tasks are split into several servers and joined again before departing the system. This model has been used for all kinds of parallel multitasking in computation and communications networks [30]. Most of the works assume that, at any time instant, tasks can be canceled and abandon their respective queue. [31] studies path redundancy in the context of cloud systems with a fork-join model, to understand the trade-off latency-computing cost. [32] analyzes the transmission of redundant requests to multiple servers for a faster execution in terms of average latency, at the cost of increased system load. It is observed that not having redundancy is optimal for highly loaded systems if service times are memoryless. The authors in [33] present a study on delay-optimal scheduling of replications in centralized and distributed multi-server systems.

There has also been some work on bounds to worst-case performance in fork-join queues, mostly concerned with the tail of the latency distribution [34]. These delay bounds concern themselves with Markovian arrival processes [35], as they model parallel or distributed processing of randomly arriving data. To the best of our knowledge, the question of delay bounds with periodic traffic, such as video or VR/AR frames, has not been investigated in either the communication or distributed processing literature.

C. Age of Information

Since the concept of AoI was introduced in the early 2010s [10], it has been the subject of intense study, being the preferred latency metric for real-time video streaming and context-aware IoT applications [36]. In these applications, the end receiver is interested in a fresh knowledge of the remotely controlled system, rather than the packet delay. Most theoretical results derive the average AoI or the PAoI. Much smaller is the number of works deriving higher moments or the full distribution of the age (see e.g. [14] [38]), although a reliable system design requires knowing the probability of occurrence of rare, but extremely damaging events.

Initial studies focused on simple queuing systems with a single node and unicast scheduled transmissions [39], [40]. However, there is already a significant number of papers addressing

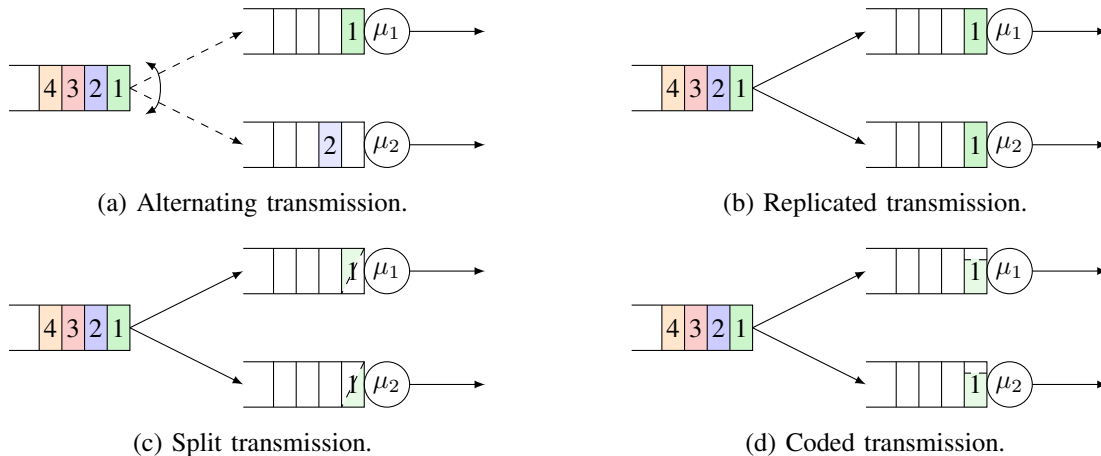


Fig. 1: Depiction of the four transmission schemes.

more complex communication scenarios and topologies, like for instance models for random access and ALOHA [41] [42], multi-cast and broadcast [43], or multi-hop transmissions [44], [45].

None of the fork-join queuing works listed in Section II-B analyzes the AoI. To the best of our knowledge, the only exceptions are [46], which gives the average age for distributed computing with k over n coding, and [47], which addresses the age-delay trade-off considering the scheduler and routing (selected path) of an M-server system with Poisson arrivals. They prove that a system designed to minimize the age will do it at the expenses of high waiting times and service times for the packets that do not contribute to the age metric (the *non-informative* packets) and the average and variance of the packet delay will therefore increase enormously.

Unlike most of the fork-related works, we do not consider removal of task in the buffers, since age-sensitive applications will typically have no feedback and there is no way for the transmitter to know when the replicas/pieces of the frame have arrived to any of the receivers.

III. SYSTEM MODEL

We consider a wireless VR system, in which rendered frames of constant size are generated with a constant period τ . The generated frames are then delivered to a user through a multipath connection using two different Radio Access Technologies (RATs). We model the two paths as two separate queuing systems with Markovian service. The two paths, dubbed 1 and 2, then have exponential service times, with average rates μ_1 and μ_2 , respectively: the service time is

exponentially distributed to account for physical and medium access issues, which introduce a significant volatility in the delivery of the data. We also consider them to have infinite queues with First Come First Serve (FCFS) service. In the following, we will refer to the individual paths in the connection as “paths” or “channels” interchangeably, using “system” to indicate the overall multipath connection, which is then similar to a $D/M/2$ queue, as the arrival process is deterministic and the service process is Markovian for both servers, but the two paths have separate queues and the transmitter has a scheduler, i.e., it can choose which connection to send the data through. We assume that the two paths also function as Packet Erasure Channels (PECs), with erasure rates ε_1 and ε_2 , respectively. We define the load ρ_j on each path j as:

$$\rho_j = \frac{L\lambda_j}{\mu_j} \quad j = 1, 2, \quad (1)$$

where λ_j is the average arrival rate on the path, which depends on the scheduling process, and L is the normalized size of the packets: a full frame is considered to have $L = 1$. We consider four different scheduling strategies, which are depicted in Fig. 1:

- The *alternating* transmission scheme, shown in Fig. 1a, is a simple round-robin scheduler: odd-numbered packets are scheduled on the first path, while even-numbered ones are scheduled on the second one. In this case, the multipath connection is used to reduce the load on the two paths: the arrival rate is $\lambda_j = \frac{1}{2\tau}$ for either connection, while we have $L = 1$.
- The *replicated* transmission scheme, shown in Fig. 1b, duplicates each frames in two packets, which are sent over both paths at once. Naturally, this increases the load on the system, as we have $\lambda_j = \frac{1}{\tau}$ on either path and $L = 1$, but it also provides error protection, as an erasure on either path can be compensated by the other replica.
- The *split* transmission scheme, shown in Fig. 1c, divides the frame in two smaller packets, each of which is sent over one path. In this case, the interarrival period is τ but the packet size is halved: we still have $\lambda_j = \frac{1}{\tau}$, but $L = 0.5$.
- The *coded* transmission scheme, shown in Fig. 1d, is a hybrid between the replicated and split schemes: the transmitter sends two packets of equal size on each path. By using MDC, each packet is decodable individually, and provides a lower-quality representation of the frame. If both packets are delivered, the video frame can be displayed at the full quality. The quality and size of each individual packet depend on the coding rate η : a value $\eta = 0.5$ corresponds to the replicated scheme, while $\eta = 1$ corresponds to the split scheme. The

arrival rate at each path is still $\lambda_j = \frac{1}{\tau}$, while we have $L = \frac{1}{2\eta}$, as the frame is encoded and then split over the two paths.

In all schemes but the first one, arrivals on the two paths are synchronized, i.e., one packet is sent on each path for each frame. Naturally, more intelligent schedulers are possible: a more advanced version of the alternating scheme would schedule the frame based on the occupation of each queue, always sending packets on the less congested path. However, this kind of scheduler is difficult to study analytically, and we will only provide simulation results for it. We can also think of an adaptive coded scheme, which changes the MDC coding rate depending on the state of the two queues, but this is beyond the scope of this work, where we aim to study the basic features of the four alternatives from Fig. 1.

In the following, we will represent random variables using capital letters, and their values with lower-case letters. Vectors are represented in bold. We define the state of the overall system when the i -th frame is generated as $\mathbf{Q}_i = (Q_{i,1}, Q_{i,2})$, where $Q_{i,j}$ represents the number of packets in channel j , including the one in service. We derive next the system time and peak age distributions for the four transmission schemes, first for the alternating scheme, then for the coding-based ones.

IV. ANALYSIS: ALTERNATING TRANSMISSION

In this scheme, packets are divided between the two paths in a round-robin fashion. In this case, the system is simple: each of the two paths is independent from the other and can be treated individually, with an arrival process with only half the rate. We can consider the error-free alternating $D/M/2$ system, in which the interarrival period for each path is 2τ . We then have the following distribution of the state $q_{i,j}$ just before an arrival, following the well-known formula derived by Erlang [48]:

$$p_{Q_{i,j}}(q_{i,j}) = (1 - \sigma_j)\sigma_j^{q_{i,j}}, \quad (2)$$

where the parameter σ_j is the solution in $(0, 1)$ to the following equation:

$$x = e^{2\mu_j\tau(x-1)}. \quad (3)$$

The existence of σ_j is guaranteed if the paths are stable, i.e., if $\rho_j = \frac{1}{2\mu_j\tau} < 1 \forall j \in \{1, 2\}$. Since the two paths can be treated as independent, the Probability Density Function (PDF) of the system time $T_{i,j}$ for a successfully received packet on path j , is given by:

$$p_{T_{i,j}}(t) = \mu_j(1 - \sigma_j)e^{-\mu_j(1-\sigma_j)t}u(t). \quad (4)$$

The PDF of the system time T_1^{alt} for successfully received packets is then given by:

$$p_{T_1^{\text{alt}}}(t) = \sum_{q_{1,1}=0}^{\infty} (1 - \sigma_1) \sigma_1^{q_{1,1}} \frac{\mu_1^{q_{1,1}+1} t^{q_{1,1}} e^{-\mu_1 t}}{q_{1,1}!}, \quad (5)$$

and the same goes for $p_{T_1^{\text{alt}}}(t)$, with inverted indices. Solving the series, we get:

$$p_{T_i^{\text{alt}}}(t) = \begin{cases} (1 - \sigma_1) \mu_1 e^{-\mu_1(1-\sigma_1)t} & \text{if } i \text{ is odd;} \\ (1 - \sigma_2) \mu_2 e^{-\mu_2(1-\sigma_2)t} & \text{if } i \text{ is even.} \end{cases} \quad (6)$$

If we take a random packet, we will simply get:

$$p_{T^{\text{alt}}}(t) = \frac{p_{T_1^{\text{alt}}}(t) + p_{T_2^{\text{alt}}}(t)}{2}. \quad (7)$$

For the AoI calculation, it is convenient to work with the probability of a packet being relevant, i.e., a successive packet has not arrived before it. We calculate first the case without channel errors. If i is odd, the probability $p_{r,1}$ that packet i is relevant is given by:

$$\begin{aligned} p_{r,1} &= P_{T_1}(\tau) + \int_{\tau}^{\infty} p_{T_1}(t) (1 - P_{T_2}(t - \tau)) dt \\ &= 1 - e^{-\mu_1(1-\sigma_1)\tau} \left(1 - \frac{\mu_1(1-\sigma_1)}{\mu_1(1-\sigma_1) + \mu_2(1-\sigma_2)} \right). \end{aligned} \quad (8)$$

The same is true for $p_{r,2}$, with inverted indices. The distribution of the peak age when a relevant packet arrives from path 1 is then:

$$\begin{aligned} p_{\Delta,1}(\delta) &= \frac{(1 - \sigma_1)}{p_{r,1}} u(\delta - \tau) \mu_1 e^{-\mu_1(1-\sigma_1)(\delta-\tau)} \left[u(2\tau - \delta) (1 - e^{-\mu_2(1-\sigma_2)\delta}) \right. \\ &\quad + u(\delta - 2\tau) \left(e^{-\mu_2(1-\sigma_2)(\delta-\tau)} e^{\mu_1(1-\sigma_1)\tau} + (1 - e^{-2\mu_2(1-\sigma_2)\tau}) e^{-\mu_2(\delta-2\tau)} \right. \\ &\quad \left. \left. + \frac{(1 - \sigma_2)}{\sigma_2} e^{-\mu_2\delta} (e^{\mu_2\sigma_2\delta} - e^{2\mu_2\sigma_2\tau}) \right) \right]. \end{aligned} \quad (9)$$

The unconditioned PAoI distribution is:

$$p_{\Delta^{\text{alt}}}(\delta) = \frac{p_{r,1} p_{\Delta,1}(\delta) + p_{r,2} p_{\Delta,2}(\delta)}{p_{r,1} + p_{r,2}}. \quad (10)$$

If we consider error-prone channels, the exact PAoI distribution is hard to compute, as we need to consider all possible orderings of past packets. We then compute a lower bound, assuming that, for the transmission of packet i , packet $i - 3$ has already arrived at the other path, i.e., multiple packets can be lost, but we never have more than 2 consecutive packets arrive out-of-order. This approximation is tight for low traffic scenarios. We denote the number of consecutive failures as F . If the number of consecutive failures is larger than 1, the bound is given by:

$$p_{\Delta_1^{\text{alt},e|F}}(\delta|f) = p_{T_1|r_1}(\delta - (f + 1)\tau) \forall f \geq 1, \quad (11)$$

where the conditioned PDF $p_{T_1|r_1}(t)$ is given by:

$$p_{T_1|r_1}(t) = \frac{\mu_1(1 - \sigma_1)e^{-\mu_1(1-\sigma_1)t}(\varepsilon_2 + (1 - \varepsilon_2)(1 + u(t - \tau)(e^{-\mu_2(1-\sigma_2)(t-\tau)} - 1))}{\varepsilon_2 + (1 - \varepsilon_2)p_{r,1}}. \quad (12)$$

The same is true for the second path, after inverting the indices. We can then compute $p_{\Delta^{\text{alt},e}}$ by using the law of total probability:

$$p_{\Delta^{\text{alt},e}}(\delta) = \frac{(1 - \varepsilon_1) \left((1 - \varepsilon_2)p_{r,1}p_{\Delta_1}(\delta) + \sum_{f=1}^{\lfloor \frac{\delta}{\tau} \rfloor} p_{T_1|r_1}(\delta - (f+1)\tau)\varepsilon_1^{\lfloor f2 \rfloor} \varepsilon_2^{\lfloor f2 \rfloor} \right)}{(1 - \varepsilon_1)(\varepsilon_2 + (1 - \varepsilon_2)p_{r,1}) + (1 - \varepsilon_2)(\varepsilon_1 + (1 - \varepsilon_1)p_{r,2})} \\ + \frac{(1 - \varepsilon_2) \left((1 - \varepsilon_1)p_{r,2}p_{\Delta_2}(\delta) + \sum_{f=1}^{\lfloor \frac{\delta}{\tau} \rfloor} p_{T_2|r_2}(\delta - (f+1)\tau)\varepsilon_1^{\lfloor f2 \rfloor} \varepsilon_2^{\lfloor f2 \rfloor} \right)}{(1 - \varepsilon_1)(\varepsilon_2 + (1 - \varepsilon_2)p_{r,1}) + (1 - \varepsilon_2)(\varepsilon_1 + (1 - \varepsilon_1)p_{r,2})}. \quad (13)$$

V. ANALYSIS: MULTIPATH TRANSMISSION

In a synchronized $D/M/2$ system, frames arrive simultaneously at both paths with constant interarrival period τ . This scenario can represent a multipath transmission, using a split, replicated, or coded approach, and the three approaches differ only by the coding rate η . The steady-state distribution for this kind of system was derived in [49] following Palm probability theory [50]. The joint distribution of \mathbf{Q} , considering the overall system just before packet i is generated, is given by:

$$p_{\mathbf{Q}_i}(\mathbf{q}_i) = (1 - \sigma_1)(1 - \sigma_2)\sigma_1^{q_{i,1}}\sigma_2^{q_{i,2}}, \quad (14)$$

where σ_j is defined, like in (3), as the solution in $(0, 1)$ of the following equation:

$$x = e^{2\eta\mu_j\tau(x-1)}. \quad (15)$$

Naturally, the stability condition is now $\rho_j = \frac{1}{2\eta\mu_j\tau} < 1 \forall j \in \{1, 2\}$. In the following, we compute the distribution of the system time for the first and last packet to arrive, which will be used for the system time calculation for the three multipath schemes.

A. Minimum System Time Distribution (Error-Free)

We now consider the i -th generated request, which causes two packets to arrive simultaneously at both paths at time g_i . The two packets will then arrive at the receiver at times $r_{i,1}$ and $r_{i,2}$, depending on the system time of the two paths. We consider the minimum system time T_i^{\min} , i.e., the system time of the first packet to be received:

$$T_i^{\min} = \min_{j \in \{1,2\}} r_{i,j} - g_i. \quad (16)$$

The minimum system time is then a random variable whose distribution is the minimum between the distributions of the two independent paths. This corresponds to the delay for a successful transmission in a replicated scheme, as the first copy of the frame to arrive is decoded and shown to the user.

We first solve the following series, which is used several times in the derivation of the system time PDF. As the factor σ is guaranteed to be in the open interval $(0, 1)$ due to the stability condition on the two paths, its geometric series converges and the inversion of the two summations is possible:

$$\begin{aligned} \sum_{q=1}^{\infty} \sigma^q \sum_{n=0}^q \frac{\alpha^n}{n!} &= \sum_{q=1}^{\infty} \sigma^q + \sum_{n=1}^{\infty} \frac{\alpha^n}{n!} \sum_{q=n-1}^{\infty} \sigma^q \\ &= \frac{1}{1-\sigma} + \sum_{n=1}^{\infty} \frac{(\alpha\sigma)^n}{(1-\sigma)n!} \\ &= \frac{e^{\alpha\sigma}}{1-\sigma} - 1. \end{aligned} \quad (17)$$

We can now compute the conditioned PDF of the system time distribution, considering the system state \mathbf{q}_i as known. In the following, we omit the index of the packet i for the sake of readability. We then distinguish four cases, depending on whether each queue is empty. In the first case, the two paths are empty, and the system time is the minimum between the service times at the two paths, which are two independent exponentially distributed random variables:

$$\begin{aligned} p_{T^{\min}|\mathbf{Q}}(t|(0, 0)) &= p_{T_1|Q_1}(t|0)(1 - P_{T_2|Q_2}(t|0)) + (1 - P_{T_1|Q_1}(t|0))p_{T_2|Q_2}(t|0) \\ &= 2\eta(\mu_1 + \mu_2)e^{-2\eta(\mu_1 + \mu_2)t}u(t). \end{aligned} \quad (18)$$

In the second case, in which the first path is empty but the second has at least one packet in the queue, the system time is the minimum between an exponentially distributed random variable and an Erlang distributed one:

$$\begin{aligned} p_{T^{\min}|\mathbf{Q}}(t|(0, q_2)) &= p_{T_1|Q_1}(t|0)(1 - P_{T_2|Q_2}(t|q_2)) + (1 - P_{T_1|Q_1}(t|0))p_{T_2|Q_2}(t|q_2) \\ &= \left[e^{-2\eta\mu_1 t} \frac{(2\eta\mu_2)^{q_2+1} t^{q_2} e^{-2\eta\mu_2 t}}{q_2!} + 2\eta\mu_1 e^{-2\eta\mu_1 t} \sum_{n=0}^{q_2} \frac{(2\eta\mu_2 t)^n e^{-2\eta\mu_2 t}}{n!} \right] u(t). \end{aligned} \quad (19)$$

The third case, in which the second time is empty but the first one is not, is symmetrical to the second case, and the conditioned PDF in this case is given by (19), inverting the indices of

the two paths. Finally, if both paths have packets in the queue, the resulting distribution is the minimum between two Erlang distributed variables:

$$\begin{aligned}
p_{T^{\min}|\mathbf{Q}}(t|(q_1, q_2)) &= p_{T_1|Q_1}(t|q_1)(1 - P_{T_2|Q_2}(t|q_2)) + (1 - P_{T_1|Q_1}(t|q_1))p_{T_2|Q_2}(t|q_2) \\
&= \left[\frac{(2\eta\mu_2)^{q_2+1}t^{q_2}e^{-2\eta\mu_2t}}{q_2!} \sum_{n=0}^{q_1} \frac{(2\eta\mu_1t)^n e^{-2\eta\mu_1t}}{n!} \right. \\
&\quad \left. + \frac{(2\eta\mu_1)^{q_1+1}t^{q_1}e^{-2\eta\mu_1t}}{q_1!} \sum_{n=0}^{q_2} \frac{(2\eta\mu_2t)^n e^{-2\eta\mu_2t}}{n!} \right] u(t).
\end{aligned} \tag{20}$$

We now apply the law of total probability to remove the condition on Q_2 , using the solution of the series in (17):

$$\begin{aligned}
p_{T^{\min}|Q_1}(t|q_1) &= \sum_{q_2=0}^{\infty} \frac{p_{\mathbf{Q}}((q_1, q_2))}{\sum_{k=0}^{\infty} p_{\mathbf{Q}}((q_1, k))} p_{T^{\min}|\mathbf{Q}}(t|(q_1, q_2)) \\
&= u(t)(1 - \sigma_2) \sum_{q_2=0}^{\infty} \sigma_2^{q_2} \left[\frac{(2\eta\mu_2)^{q_2+1}t^{q_2}e^{-2\eta\mu_2t}}{q_2!} \sum_{n=0}^{q_1} \frac{(2\eta\mu_1t)^n e^{-2\eta\mu_1t}}{n!} \right. \\
&\quad \left. + \frac{(2\eta\mu_1)^{q_1+1}t^{q_1}e^{-2\eta\mu_1t}}{q_1!} \sum_{n=0}^{q_2} \frac{(2\eta\mu_2t)^n e^{-2\eta\mu_2t}}{n!} \right] \\
&= u(t)(1 - \sigma_2)e^{-2\eta(\mu_1+\mu_2)t} \left[2\eta\mu_2 e^{2\eta\mu_2\sigma_2 t} \sum_{n=0}^{q_1} \frac{(2\eta\mu_1t)^n}{n!} + \frac{(2\eta\mu_1)^{q_1+1}t^{q_1}}{q_1!} \frac{e^{2\eta\mu_2\sigma_2 t}}{1 - \sigma_2} \right].
\end{aligned} \tag{21}$$

Finally, we remove the condition on Q_1 using the same principles and get the unconditioned PDF of the minimum system time:

$$\begin{aligned}
p_{T^{\min}}(t) &= \sum_{q_1=0}^{\infty} p_{T^{\min}|Q_1}(t|q_1)p_{\mathbf{Q}_1}(q_1) \\
&= u(t)e^{-2\eta(\mu_1+\mu_2)t}(1 - \sigma_1)(1 - \sigma_2) \sum_{q_1=0}^{\infty} \sigma_1^{q_1} e^{2\eta\mu_2\sigma_2 t} \left[2\eta\mu_2 \sum_{n=0}^{q_1} \frac{(2\eta\mu_1t)^n}{n!} + \frac{(2\eta\mu_1)^{q_1+1}t^{q_1}}{(1 - \sigma_2)q_1!} \right] \\
&= u(t)2\eta [\mu_1(1 - \sigma_1) + \mu_2(1 - \sigma_2)] e^{-2\eta(\mu_1(1-\sigma_1)+\mu_2(1-\sigma_2))t}.
\end{aligned} \tag{22}$$

As stated above, the minimum system time T^{\min} can represent the latency of a replicated packet sent over multiple connections, only one copy of which needs to be delivered in order to fulfill the request. It is interesting to note that the resulting system time is still exponentially distributed, with parameter $2\eta(\mu_1(1 - \sigma_1) + \mu_2(1 - \sigma_2))$. The Cumulative Density Function (CDF) of the system time distribution is then given by:

$$P_{T^{\min}}(t) = u(t)(1 - e^{-2\eta(\mu_1(1-\sigma_1)+\mu_2(1-\sigma_2))t}). \tag{23}$$

B. Minimum System Time Distribution (Error-Prone)

We can now consider a more interesting scenario, in which the two channels are error-prone and behave as independent PECs with packet erasure probability ε_1 and ε_2 , respectively. This is a key scenario for replicated transmission, as sending two copies of a frame can protect it from channel errors as well as reducing latency. We then have a probability $p_s^{\min} = 1 - \varepsilon_1 \varepsilon_2$ of fulfilling each request. Furthermore, we define $\phi_{1,2} = \frac{(1-\varepsilon_1)(1-\varepsilon_2)}{p_s^{\min}}$, $\phi_1 = \frac{(1-\varepsilon_1)\varepsilon_2}{p_s^{\min}}$, and $\phi_2 = \frac{(1-\varepsilon_2)\varepsilon_1}{p_s^{\min}}$, to identify the probability of having a successful request with two received packet, only the packet on the first path being received, and only the packet on the second path being received, respectively. We now adjust the system time PDF calculation to account for the possibility of erasure. We denote the minimum system time with errors as $T^{\min,e}$, and divide the computation in the same four cases as above. We now consider the conditioned system time PDF when both paths are empty:

$$p_{T^{\min,e}|\mathbf{Q}}(t|(0,0)) = \phi_{1,2}p_{T^{\min}|\mathbf{Q}}(t|(0,0)) + 2\eta(\phi_1\mu_1e^{-2\eta\mu_1t} + \phi_2\mu_2e^{-2\eta\mu_2t})u(t). \quad (24)$$

In the second case, in which the first path is empty but the second has at least one packet in the queue, the conditioned system time PDF is given by:

$$p_{T^{\min,e}|\mathbf{Q}}(t|(0,q_2)) = \phi_{1,2}p_{T^{\min}|\mathbf{Q}}(t|(0,q_2)) + 2\eta\phi_1\mu_1e^{-2\eta\mu_1t}u(t) + \phi_2\frac{(2\eta\mu_2)^{q_2+1}t^{q_2}e^{-2\eta\mu_2t}}{q_2!}u(t). \quad (25)$$

As for the error-free system, the third case, in which the second time is empty but the first one is not, is symmetrical to the second case. Finally, if both paths have packets in the queue, the resulting distribution is:

$$p_{T^{\min,e}|\mathbf{Q}}(t|(q_1,q_2)) = \phi_{1,2}p_{T^{\min}|\mathbf{Q}}(t|(q_1,q_2)) + \phi_1\frac{(2\eta\mu_1)^{q_1+1}t^{q_1}e^{-2\eta\mu_1t}}{q_1!}u(t) + \phi_2\frac{(2\eta\mu_2)^{q_2+1}t^{q_2}e^{-2\eta\mu_2t}}{q_2!}u(t). \quad (26)$$

As above, we now use the law of total probability to remove the condition on Q_2 :

$$\begin{aligned} p_{T^{\min,e}|Q_1}(t|q_1) &= \sum_{q_2=0}^{\infty} \frac{p_{\mathbf{Q}}((q_1,q_2))}{\sum_{k=0}^{\infty} p_{\mathbf{Q}}((q_1,k))} p_{T^{\min,e}|\mathbf{Q}}(t|(q_1,q_2)) \\ &= (1 - \sigma_2)u(t) \left[\phi_{1,2}p_{T^{\min}|Q_1}(t|q_1) + \phi_1\frac{(2\eta\mu_1)^{q_1+1}t^{q_1}e^{-2\eta\mu_1t}}{q_1!} \right. \\ &\quad \left. + 2\eta\phi_2\mu_2e^{-2\eta\mu_2t}(e^{2\eta\mu_2\sigma_2t} - 1) \right]. \end{aligned} \quad (27)$$

Finally, we remove the condition on Q_1 using the same principles and get the unconditioned PDF of the minimum system time:

$$\begin{aligned} p_{T^{\min},e}(t) &= \sum_{q_1=0}^{\infty} p_{T^{\min},e|Q_1}(t|q_1)p_{\mathbf{Q}_1}(q_1) \\ &= \phi_{1,2}p_{T^{\min}}(t) + 2\eta(1-\sigma_1)(1-\sigma_2)u(t) \left[\phi_1\mu_1e^{-2\eta\mu_1(1-\sigma_1)t} + \phi_2\mu_2e^{-2\eta\mu_2(1-\sigma_2)t} \right]. \end{aligned} \quad (28)$$

We remind the reader that the latency above is computed only for successful requests, while a fraction $1 - p_s^{\min}$ of the frames is lost, as both copies of the packet are erased. The system time CDF in the error-prone case is given by:

$$P_{T^{\min},e}(t) = \phi_{1,2}P_{T^{\min}}(t) + u(t)2\eta \left[\phi_1(1-\sigma_2)(1 - e^{-2\eta\mu_1(1-\sigma_1)t}) + \phi_2(1-\sigma_1)(1 - e^{-2\eta\mu_2(1-\sigma_2)t}) \right]. \quad (29)$$

C. Maximum System Time Distribution

We now consider the maximum system time T_i^{\max} , i.e., the system time of the second packet to be received:

$$T_i^{\max} = \max_{j \in \{1,2\}} r_{i,j} - g_i. \quad (30)$$

In a split transmission scheme, the maximum system time corresponds to the delay of a successful frame. As for T_i^{\min} , the distribution of T_i^{\max} is the maximum of the two distributions of the system times at the two paths, which are independent if the state of the two queues is given. The distribution we compute below is only for successful requests, which in this case require both packets to be delivered: we have $p_s^{\max} = (1 - \varepsilon_1)(1 - \varepsilon_2)$. The value of σ_j is given by (15). As above, we omit the index of the request i for brevity, and consider four different cases based on the state of the two queues immediately before the request. In the first case, both queues are empty, and the delay is the maximum between two exponential random variables:

$$p_{T^{\max}|\mathbf{Q}}(t|(0,0)) = 2\eta \left(\mu_1e^{-2\eta\mu_1t} + \mu_2e^{-2\eta\mu_2t} - (\mu_1 + \mu_2)e^{-2\eta(\mu_1+\mu_2)t} \right) u(t). \quad (31)$$

In the second case, the second path has at least one packet in the queue when the request arrives, while the first one is empty. In this case, the system time distribution is the maximum between an exponentially distributed random variable and an Erlang distributed one:

$$\begin{aligned} p_{T^{\max}|\mathbf{Q}}(t|(0,q_2)) &= \left[(1 - e^{-2\eta\mu_1t}) \frac{(2\eta\mu_2)^{q_2+1} t^{q_2} e^{-2\eta\mu_2t}}{q_2!} \right. \\ &\quad \left. + 2\eta\mu_1e^{-2\eta\mu_1t} \left(1 - \sum_{n=0}^{q_2} \frac{(2\eta\mu_2t)^n e^{-2\eta\mu_2t}}{n!} \right) \right] u(t). \end{aligned} \quad (32)$$

As for the minimum system time, $p_{T^{\max}|\mathbf{Q}}(t|(q_1, 0))$ follows the same distribution, inverting the indices of the two paths. Finally, we consider the case in which both paths have queued packets. In this case, the distribution of the overall system time is the maximum between two Erlang distributed variables, which correspond to the system time for the two paths:

$$p_{T^{\max}|\mathbf{Q}}(t|(q_1, q_2)) = \left(1 - \sum_{n=0}^{q_1} \frac{(2\eta\mu_1 t)^n e^{-2\eta\mu_1 t}}{n!}\right) \frac{(2\eta\mu_2)^{q_2+1} t^{q_2} e^{-2\eta\mu_2 t}}{q_2!} u(t) \\ + \frac{(2\eta\mu_1)^{q_1+1} t^{q_1} e^{-2\eta\mu_1 t}}{q_1!} \left(1 - \sum_{n=0}^{q_2} \frac{(2\eta\mu_2 t)^n e^{-2\eta\mu_2 t}}{n!}\right) u(t). \quad (33)$$

We can then use (31), (32), and (33) to remove the condition on Q_2 from the system time distribution, using the law of total probability to condition only on the first queue's state:

$$p_{T^{\max}|Q_1}(t|q_1) = \sum_{q_2=0}^{\infty} \frac{p_{\mathbf{Q}}((q_1, q_2))}{\sum_{k=0}^{\infty} p_{\mathbf{Q}}((q_1, k))} p_{T^{\max}|\mathbf{Q}}(t|(q_1, q_2)) \\ = u(t)(1 - \sigma_2) \left[2\eta\mu_2 e^{-2\eta\mu_2(1-\sigma_2)t} \left(1 - \sum_{n=0}^{q_1} \frac{(2\eta\mu_1 t)^n e^{-2\eta\mu_1 t}}{n!}\right) \right. \\ \left. + \frac{(2\eta\mu_1)^{q_1+1} t^{q_1} e^{-2\eta\mu_1 t}}{(1 - \sigma_2)q_1!} (1 - e^{-2\eta\mu_2(1-\sigma_2)t}) \right]. \quad (34)$$

We can now remove the condition on the state of the first queue as well:

$$p_{T^{\max}}(t) = \sum_{q_1=0}^{\infty} p_{T^{\max}|Q_1}(t|q_1) p_{\mathbf{Q}_1}(q_1) \\ = u(t) 2\eta \left[(1 - \sigma_1)\mu_1 e^{-2\eta\mu_1(1-\sigma_1)t} (1 - e^{-2\eta\mu_2(1-\sigma_2)t}) \right. \\ \left. + (1 - \sigma_2)\mu_2 e^{-2\eta\mu_2(1-\sigma_2)t} (1 - e^{-2\eta\mu_1(1-\sigma_1)t}) \right]. \quad (35)$$

The maximum system time represents the latency for a system which requires both packets to fulfill the request. Network coded transmissions, in which both packets contain part of the information required at the receiver, is one example of this kind of system. The CDF of the system time is:

$$P_{T^{\max}}(t) = u(t) \left[1 - e^{-2\eta\mu_1(1-\sigma_1)t} - e^{-2\eta\mu_2(1-\sigma_2)t} + e^{-2\eta(\mu_1(1-\sigma_1) + \mu_2(1-\sigma_2))t} \right]. \quad (36)$$

D. System time and PAoI for synchronized systems

After computing $p_T^{\min,e}$ and p_T^{\max} , we can go ahead and get the system time for a coded system. In the most general case, we have a coded system with $\eta \in (0.5, 1)$. We then have the following

CDF:

$$p_{T^{\text{LQ}}}(t) = p_T^{\text{min},e}(t) \quad (37)$$

$$p_{T^{\text{HQ}}}(t) = p_T^{\text{max},e}(t), \quad (38)$$

where T^{LQ} is the delay of the low-quality version of the frame and T^{HQ} is the delay of the high-quality version of the frame. The split and replicated systems are two extreme cases of the coded transmission: in the former, the low-quality frame is undecodable, and $\eta = 1$, while in the latter, the low quality version is identical to the full-quality one, and $\eta = 0.5$.

We can now consider the distribution of the PAoI, denoted by Δ , in the systems for which we just computed the system time PDF. For simplicity, we refer to the more general error-prone system, which the error-free case is a special case of with $\varepsilon_1 = \varepsilon_2 = 0$. If we have a synchronized $D/M/2$ system with success probability p_s and system time PDF $p_T(t)$ for successful packets, we need to consider the possibility of request failures. We denote the number of failures as F : if there are f consecutive failures, the PDF of the PAoI is simply given by:

$$p_{\Delta|F}(\delta|f) = p_T(\delta - (f + 1)\tau)u(\delta - (f + 1)\tau) \quad \forall f \geq 1. \quad (39)$$

This is due to the deterministic nature of the arrival process, which increases the age by τ for every failure. As failures are independently distributed and the success probability is p_s , we can now apply the law of total probability to remove the condition:

$$p_{\Delta}(\delta) = p_s \sum_{f=0}^{\lfloor \frac{\delta}{\tau} \rfloor - 1} (1 - p_s)^f p_T(\delta - (f + 1)\tau). \quad (40)$$

By substituting p_s^{min} and $p_T^{\text{min},e}$, or p_s^{max} and p_T^{max} , we can compute the distribution of the PAoI for replicated and split systems, respectively.

In a coded transmission scheme with MDC, the concept of PAoI is split between the two qualities: as above, we can substitute p_s^{min} and $p_T^{\text{min},e}$ into (40) to compute the PAoI of low-quality frames, or p_s^{max} and p_T^{max} to compute the peak age considering only high-quality frames.

VI. SIMULATION RESULTS

In this section, we compare our analytical results with an extensive Monte Carlo simulation, consisting of over 10^6 packets, in order to verify the analysis. The first 1000 packets of each simulation were cut from the results to avoid the initial transition effects and ensure that the system was only considered in a steady state. We analyzed both the system time for the four

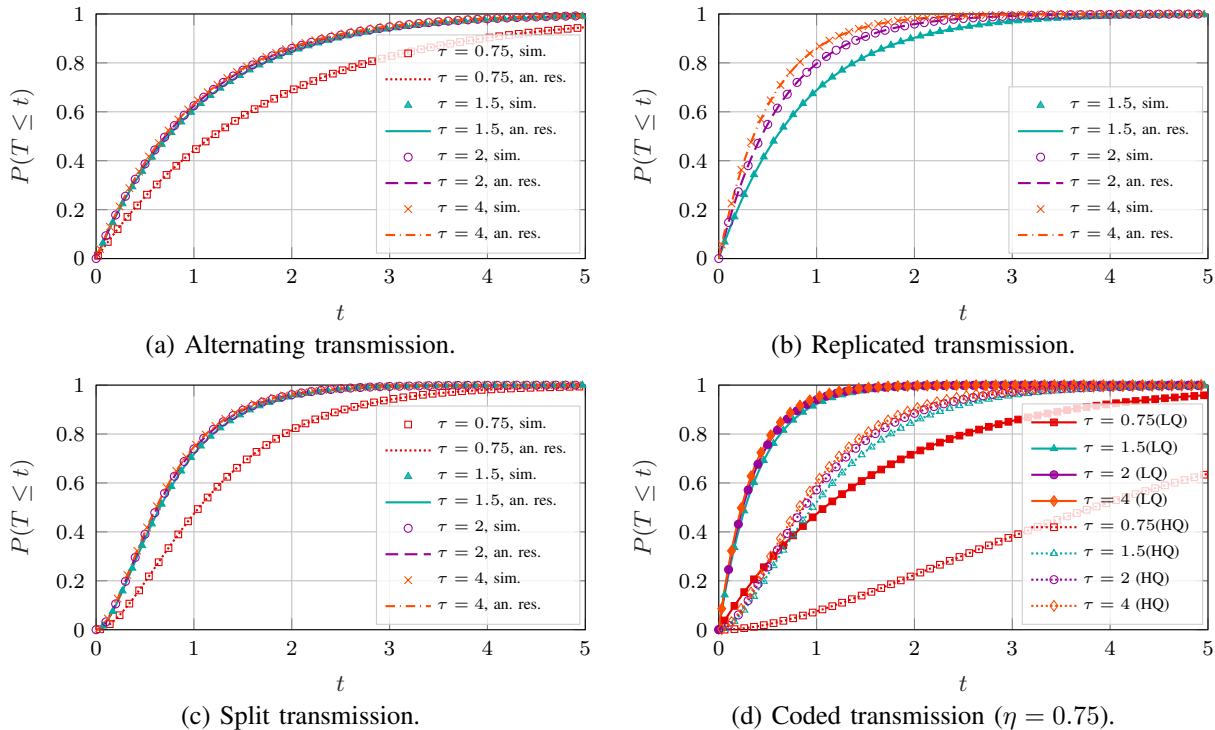


Fig. 2: Latency CDF for the four schemes in an error-free $D/M/2$ with $\mu_1 = \mu_2 = 1$.

schemes and the PAoI, considering both the full distribution and the 99th percentile, used as a proxy for the worst-case performance.

A. System time

We first look at the latency of the four schemes in an error-free system. The two paths have the same service rates, which are set to 1. Fig. 2 shows the CDF of the system time for different values of the inter-frame period τ . The alternating transmission scheme in Fig. 2a can support $\tau = 0.75$, but it has a long tail: this is due to the fact that it relies on a single system sending a large packet. The replicated scheme can avoid this problem, as shown in Fig. 2b, as its latency is the minimum between the two paths. However, the higher load it imposes on the system means that it cannot support a frame rate higher than 1 (e.g., the $\tau = 0.75$ case represented in the other schemes). This is not true for the split scheme in Fig. 2c, which has both a lower load and a light tail. While it requires both paths to deliver their packets to decode a frame, it can still have a good worst-case performance because of the reduced packet size. Finally, the coded scheme, whose performance is shown in Fig. 2d, is a compromise between replicating

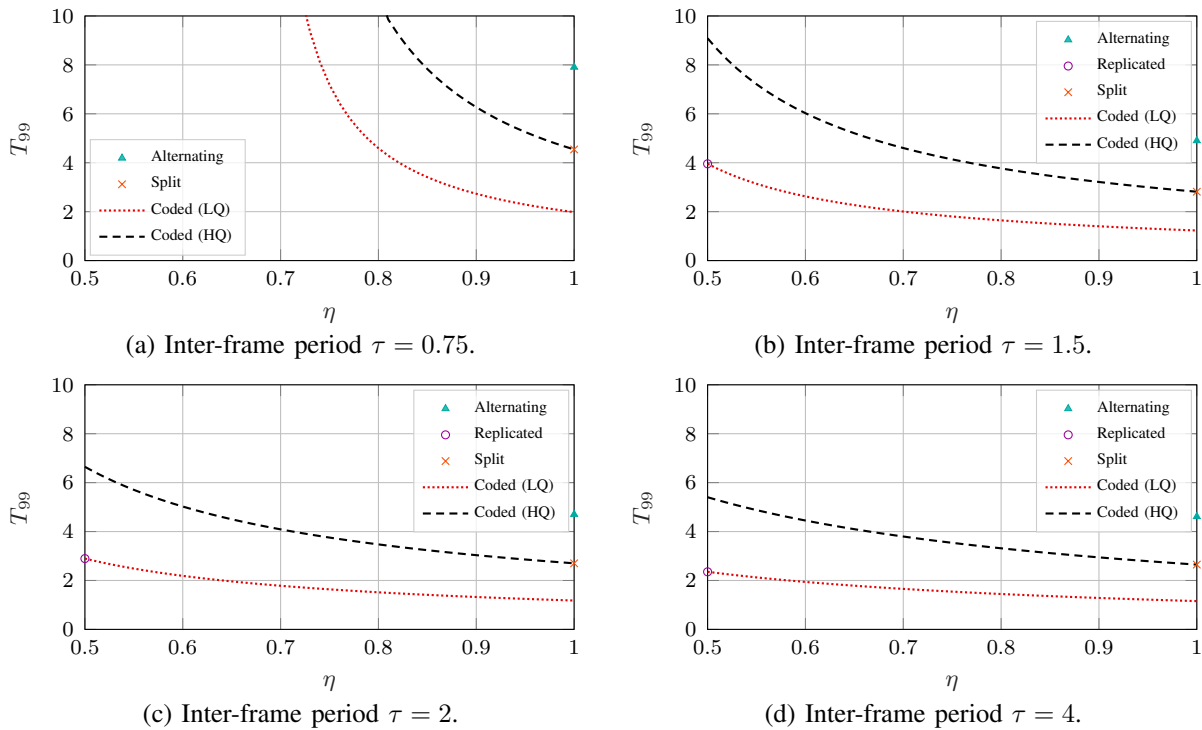


Fig. 3: 99th percentile T_{99} of the latency as a function of the coding rate η in an error-free $D/M/2$ with $\mu_1 = \mu_2 = 1$.

and splitting: it can deliver a lower-quality version of the frame much faster than the other systems, but the full-quality version has a high latency, since it requires both packets to be delivered and each packet is larger than in the split system. In this case, the high-quality curve for $\tau = 0.75$ is still in the stability region, unlike the replicated scheme, although with a long tail. As expected, the simulated results perfectly match the analytical curves. This is also true for the coded transmission, but Fig. 2d does not show the Monte Carlo results to improve clarity.

Naturally, the coded system depends on the efficiency of the code: an MDC scheme with a higher η will have smaller packets, but each individual packet will contain less information on the frame, so the lower-quality version will have a worse quality than the equivalent for a scheme with a smaller η . The replicated and split scheme are the two extremes: in the replicated scheme, each packet is enough on its own to get the full-quality frame, while in the split scheme, an individual packet is not enough to decode the frame at any quality. Fig. 3 shows the worst-case latency performance of the scheme, represented using the 99th percentile of the system time, along with the three other schemes. We have $\eta = 1$ for the alternating and split schemes, and

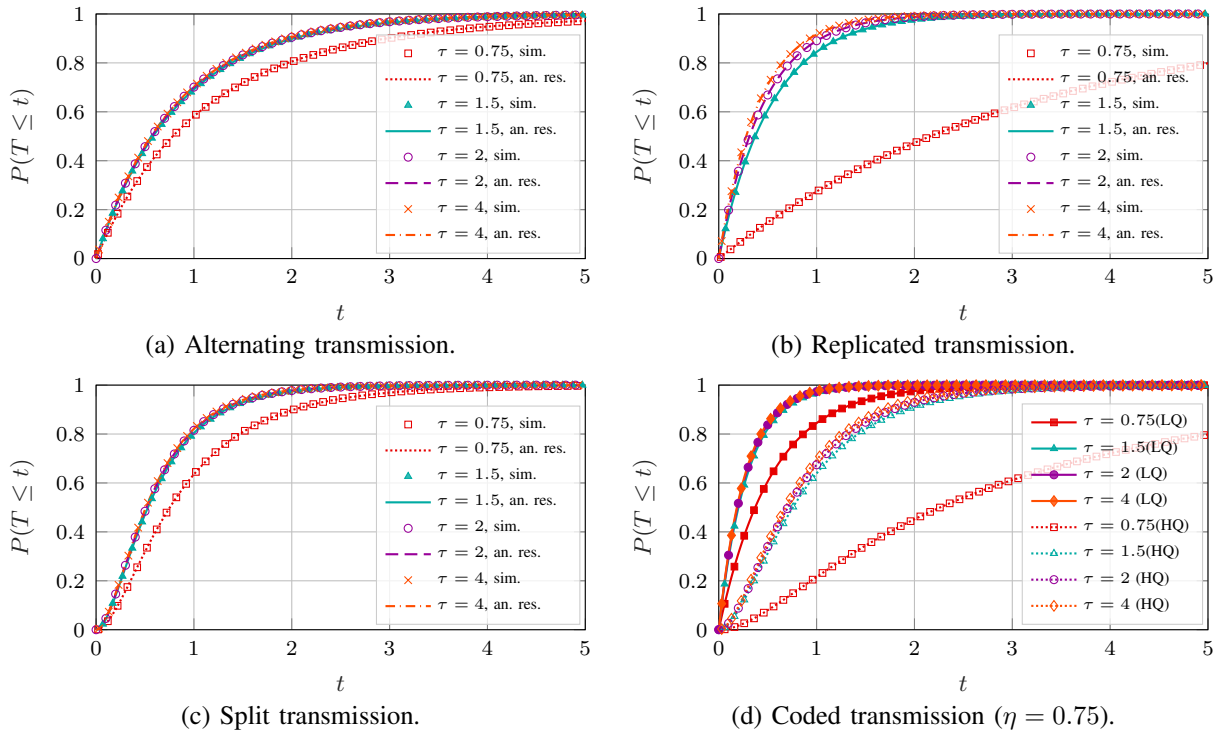


Fig. 4: Latency CDF for the four schemes in an error-free $D/M/2$ with $\mu_1 = 1$ and $\mu_2 = 1.5$.

$\eta = 0.5$ for the replicated scheme. As the plots show, there is an inverse relationship between the latency performance and the quality achievable with just one packet, as increasing the redundancy leads to a sharp increase in the latency, and the system can become unstable if packets are both frequent and large, as is shown in Fig. 3a, which has $\tau = 0.75$. In this case, the load on the two paths is already high, so choosing a low η can increase the queuing delay significantly, with a significant delay increase. If the two paths have a very low load, as in Fig. 3d, which has $\tau = 4$, the benefits from a more efficient code are smaller, and the latency cost of having a higher quality from a single packet is lower.

We can then look at what happens in an unbalanced system, in which the two paths have different service rates: Fig. 4 shows the CDF of the latency for the four schemes in a system with $\mu_1 = 1$ and $\mu_2 = 1.5$. In this case, the schemes that can rely on the faster path to transmit the frame, i.e., the replicated and coded schemes, can significantly improve their performance, while the tail of the distribution for the alternating scheme remains similar to the balanced case: packets on the slower path can still have long delays. The same thing happens for the split system, for which the slower path is still a limiting factor: while performance is slightly better

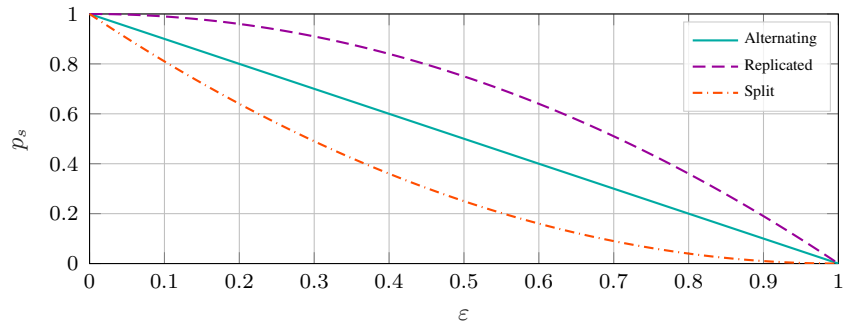


Fig. 5: Frame delivery probability as a function of ε in an error-prone $D/M/2$ with $\varepsilon_1 = \varepsilon_2 = \varepsilon$.

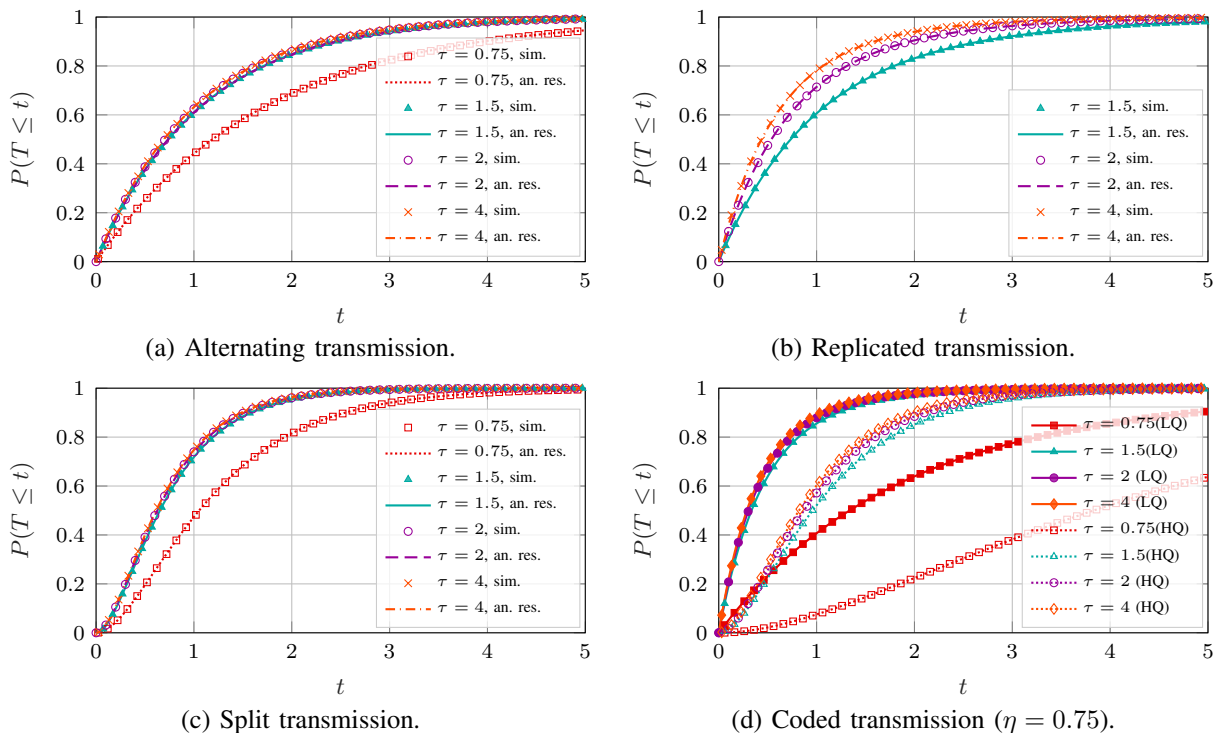


Fig. 6: Latency CDF for the four schemes in an error-prone $D/M/2$ with $\mu_1 = \mu_2 = 1$ and $\varepsilon_1 = \varepsilon_2 = 0.2$.

than in the balanced scenario, the improvements are far smaller than the one of the replicated system. We note that alternating scheme can benefit from a certain adaptation when the service rates are unbalanced; for example, one possibility could be to try to keep the load on each of the channels equal.

Finally, we consider what happens in an error-prone system, as the transmission schemes

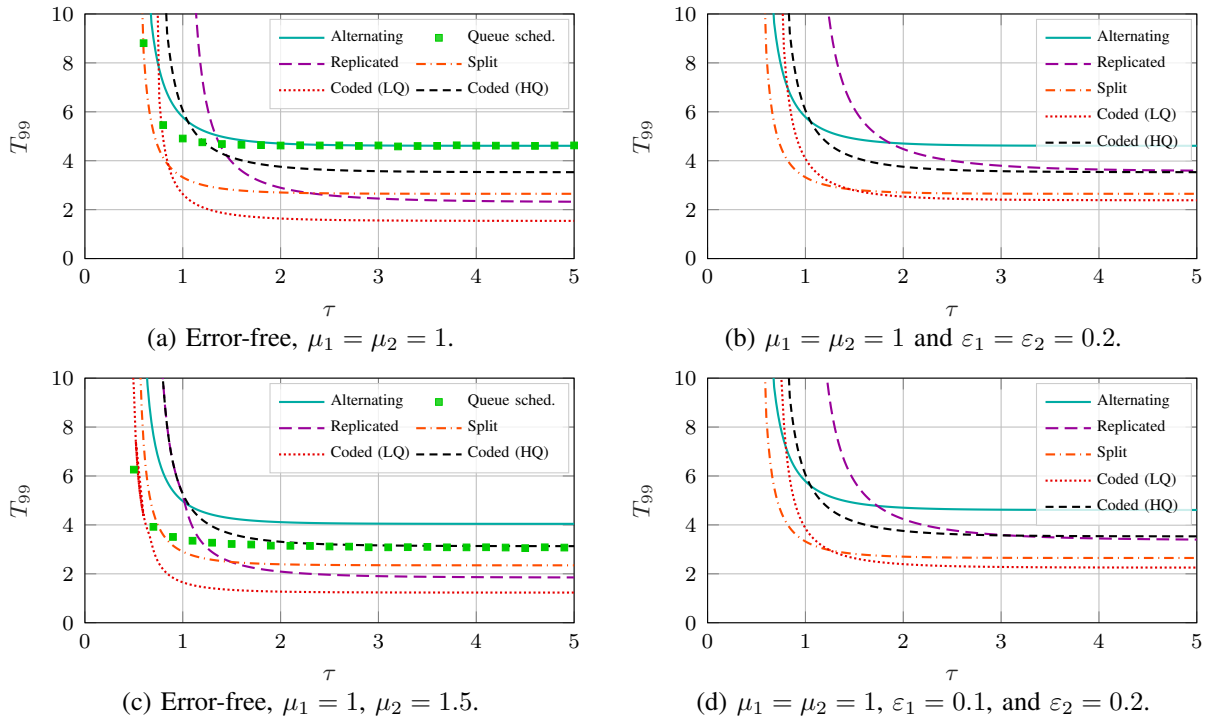


Fig. 7: 99th percentile T_{99} of the latency as a function of the inter-frame time in a $D/M/2$. The coded transmission has $\eta = 0.75$.

provide different protection from errors. While the replicated scheme provides extra redundancy by duplicating the packet, the alternating one provides no protection at all against packet erasures, while the split scheme does even worse. In order for a frame to be decoded in the split scheme, both halves need to be delivered to the receiver. Fig. 5 shows the frame decoding probability as a function of the packet erasure probability (considering the same erasure probability on both paths): as expected, the replicated scheme is much more reliable, and the split scheme is less so, while the alternating scheme follows the erasure probability exactly. In the coded scheme, the probability of decoding a frame at any quality is the same as for the replicated scheme, while the probability of getting a full-quality frame follows the curve for the split system, as it requires both path to deliver their part correctly.

This difference between the schemes is reflected in the CDF of the latency of successfully delivered frames, which is shown in Fig. 6 for a system with $\mu_1 = \mu_2 = 1$ and $\varepsilon_1 = \varepsilon_2 = 0.2$. In this case, the distributions for the alternating and split scheme, as well as for the high-quality version of the coded transmission, are exactly the same as in Fig. 2. This is because any packet

loss causes the whole frame to be lost, and is then not computed in the latency distribution. On the other hand, the replicated scheme and the low-quality version of the coded transmission have a higher delay: this is because they can recover from errors on one path by using the other, but cannot then use the benefits of path diversity to improve latency. In general, the far lower error rate of these schemes makes them preferable in systems with a high packet erasure probability.

We can also look at system optimization, if we have an application that can work at different frame rates: Fig. 7 shows the 99th percentile of the latency as a function of τ for 4 different systems. As expected, a longer inter-frame time leads to a reduced latency in all cases: as the load on the system decreases, the probability of having to wait for the queued frames to be sent becomes smaller. The alternating system, which does not exploit the parallel paths fully, can support a high frame rate but performs worse than the other systems when the load is low (the 99th percentile of the service time, with $\mu = 1$, would be equal to $-\log(0.01) \simeq 4.6$). On the other hand, the replicated system has a very high load, and underperforms for low values of τ , but can actually keep a low latency when the load on the system is low. The split system provides a middle ground, but it is also highly vulnerable to errors, as previously discussed. Finally, the MDC solution can provide a very good delay, smaller than all the other schemes', for the low-quality version, while still delivering the full-quality frame in a reasonable time. We also provide the simulation results for a queue-based scheduler, which transmits the packet over the path with the shortest queue, in the two error-free scenarios. As expected, a pure round-robin scheduler like the alternating scheme underperforms in the unbalanced scenario, but it actually performs very well in the balanced one, except for very high frame rates. This is because the two paths will have a similar queue most of the time, so the alternating scheme is close to the optimal uncoded scheme if the load is relatively low.

B. Peak Age of Information

We now analyze the PAoI performance of the four schemes. We first look at the simple error-free, balanced system with two paths with the same service rate. Fig. 8 shows the CDF of the PAoI for the four schemes. Unlike the system time, PAoI does not necessarily benefit from a lower load on the system, as it also includes the inter-frame time: the scenario with $\tau = 4$ has the worst PAoI for all four schemes. It is interesting to note that the CDF for the alternating scheme, shown in Fig. 8a, is not smooth: this is because in some cases frame i arrives before frame $i - 1$, which is transmitted on the other path. This out-of-order arrival can only result

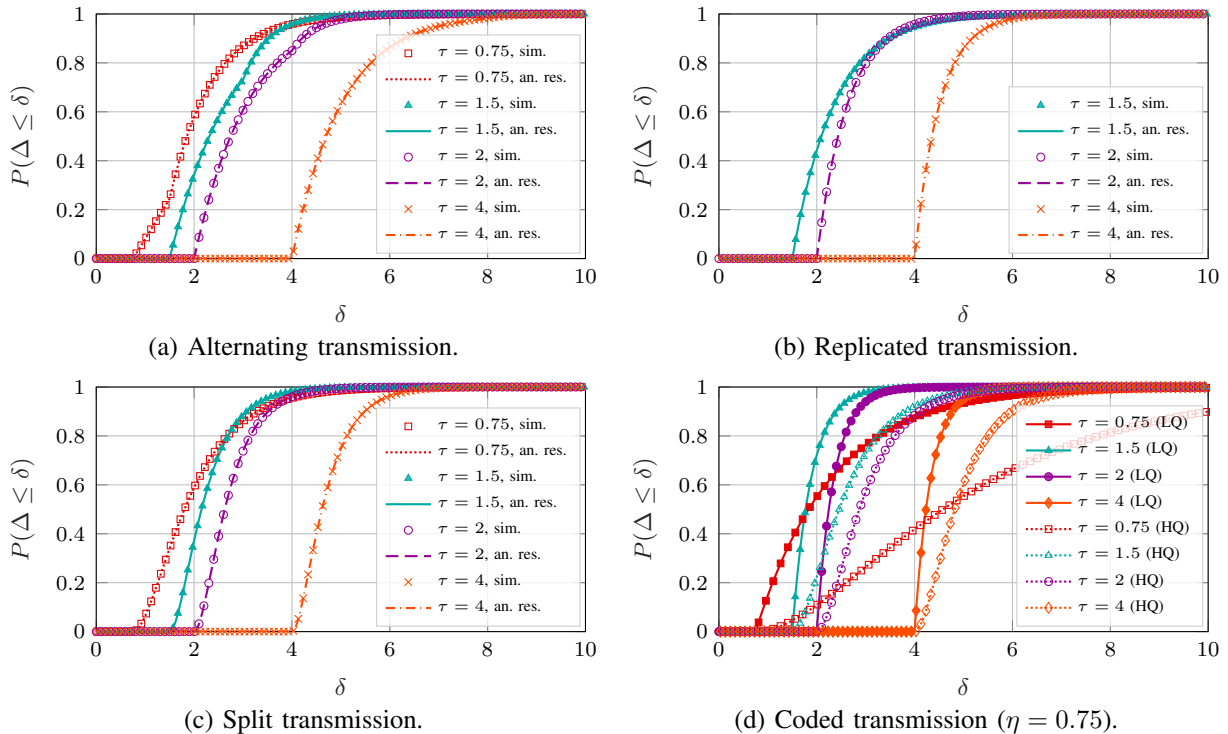


Fig. 8: PAoI distribution for the three schemes in an error-free $D/M/2$ with $\mu_1 = \mu_2 = 1$. The coded transmission has $\eta = 0.75$.

in a PAoI of at least 2τ , as the age of the $i - 2$ -th frame, which has certainly arrived before the i -th as it was sent on the same path, is 2τ when the i -th frame is sent. Interestingly, the CDFs for different values of τ also cross, which is an indication that systems optimized for the average PAoI will not have optimal worst-case performance. This is also true for the replicated and split schemes, which have similar PAoI distributions, as shown in Fig. 8b and Fig. 8c. As for the latency, the coded scheme, shown in Fig. 8d, can outperform all others and deliver the lower-quality version with a significantly lower PAoI, while the full-quality version is somewhat slower in most cases. The coded scheme also has a case with very high load, for $\tau = 0.75$, which is close to its stability limit: in this case, the load on the system is too high and the PAoI performance is not good. This further highlights the need to optimize the frame rate, as setting the wrong frame rate can significantly increase the PAoI, consequently decreasing the QoE of the VR service.

As we discussed in Sec. IV, we do not compute the precise CDF of the PAoI of the alternating scheme in a scenario with errors, as we do not consider the possibility of multiple out-of-order

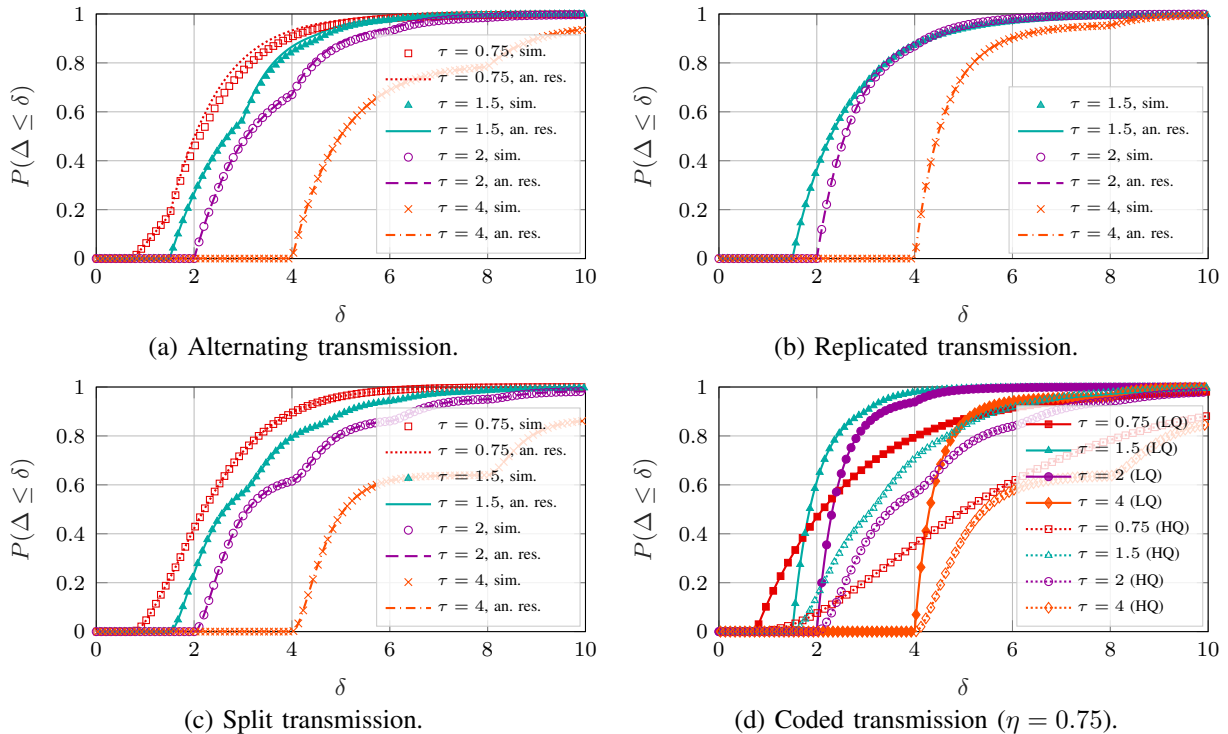


Fig. 9: PAoI distribution for the three schemes in an error-prone $D/M/2$ with $\mu_1 = \mu_2 = 1$ and $\varepsilon_1 = \varepsilon_2 = 0.2$. The coded transmission has $\eta = 0.75$.

packets, which can further increase the age. Fig. 9, which shows the CDF of the peak age in an error-prone system in which both channels have an error rate of 0.2, shows this: in Fig. 9a, the actual age is higher than the bound. The bound is tighter for low system loads, and there are now multiple flection points that correspond to successive errors in the transmission. The errors also cause flection points in Fig. 9b, and the tail of the age is shifted to the right because of packet loss. This phenomenon is much worse for the split scheme, as shown in Fig. 9c, as the split system is much more vulnerable to errors. This can cause the PAoI to increase significantly. The same is true for the full-quality PAoI of the coded scheme, as depicted in Fig. 9d, while the lower-quality version of the frames can actually be delivered with a relatively low PAoI even with a high error rate.

We now look at the optimization of the system, using the 99th percentile of the PAoI as a metric for the worst-case performance. Fig. 10 shows what happens as we change τ for the four considered schemes. All results have a U shape, with an optimal frame rate which balances the inter-frame period and the latency of frames that are sent. Naturally, this optimal point is

different for different schemes and scenarios. However, it is interesting to note that the lower-quality version of the coded scheme always has the lowest age, aside from having the lowest frame loss. On the other hand, the replicated scheme always performs slightly worse than the split scheme, as even though it will lose fewer frames, its higher load significantly increases the optimal inter-frame period. We can also see that the real age for the alternating system is close to the bound for the plots with error (shown on the right). The alternating scheme can perform slightly better than the split scheme, but is outperformed by the coded scheme at the lower quality. On the other hand, the full-quality version of the coded frames has a very high age, as it has no protection from errors and the higher load associated to the redundancy in the MDC scheme. In general, the alternating scheme performs surprisingly well in terms of PAoI. All the schemes could benefit from a more advanced scheduler, regulating the load on the two paths based on the number of packets still in the queue: unlike latency-oriented systems, which should have a very low load (and, consequently, little effect from improving the scheduler, as the queues are almost always empty), PAoI is minimized for rather high load values, close to 0.5, so having an intelligent scheduler can be a significant improvement.

As we did for the system time, we can then analyze the effect of the coding rate on the 99th percentile of the PAoI in the coded scheme, as shown in Fig. 11. In this case, we have used an optimized frame rate, i.e., set the inter-frame period that minimizes the 99th percentile of the PAoI for each value of η . The two plots on the left, whose scenarios are error-free, show a smaller effect of the coding rate, while it becomes more important for error-prone system. The intuitive understanding that we got from the system time results holds: the more stressed a system is, the more an efficient code matters, and the tighter the trade-off between quality and latency or age becomes. However, while latency-oriented systems are very sensitive to load, PAoI is very sensitive to the packet erasure probability, as missing a frame can significantly increase the age. The results for the queue-based scheduler are also shown for the two error-free scenarios: in this case, the alternating scheme performs almost as well even in the unbalanced scenario. This is because sending multiple consecutive packets over the same path might improve the average age, but has a negative effect in the worst case, as one hold-up can block two consecutive packets, increasing the age significantly.

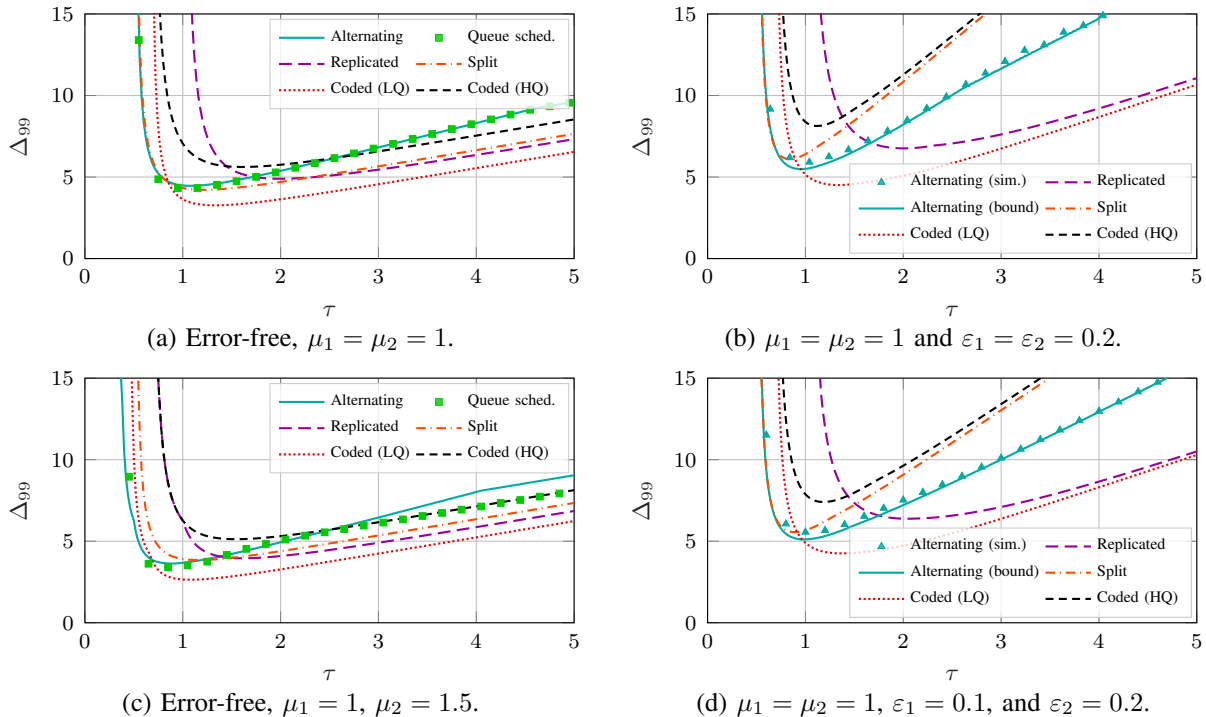


Fig. 10: 99th percentile Δ_{99} of the PAoI as a function of the inter-frame time in a $D/M/2$. The coded transmission has $\eta = 0.75$.

VII. CONCLUSIONS AND FUTURE WORK

In this work, we analyzed some schemes for the transmission of data over parallel queuing systems, with multipath VR as a motivating scenario. Unlike previous works on the fork-join model, we derived the full distribution of the latency and PAoI for uncoded and coded schemes in the presence of communication errors, and examined the performance of the various schemes as a function of the frame rate and the efficiency of the video encoding. The trade-offs between picture quality, frame rate, and timeliness are complex, and our analysis provides a handy tool for system designers.

The analysis opens several avenues of future research, most of which aim at making the model more realistic. The use of more complex communication models and scheduling schemes is one, while another is a closer examination of real omnidirectional video codecs and traffic models. These two expansions of the work can be combined to reach a realistic scheduling framework, which should also take into account the human perception of smoothness and delay in VR.

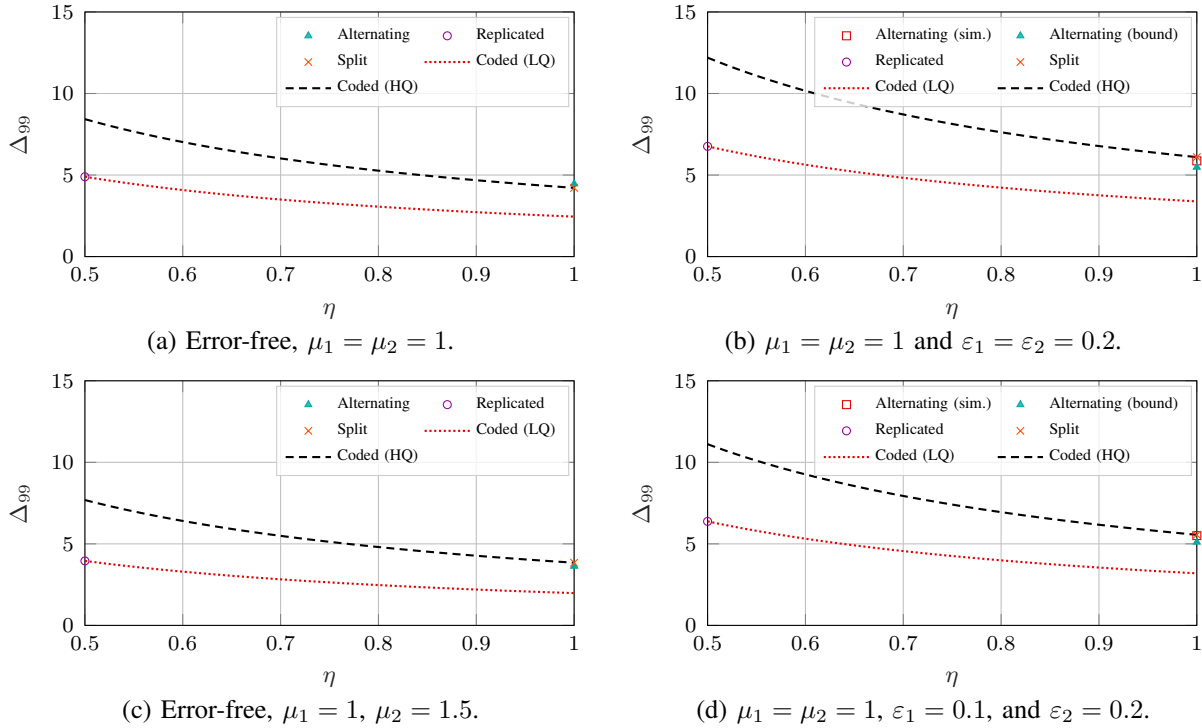


Fig. 11: 99th percentile Δ_{99} of the PAoI with optimized frame rate as a function of the coding rate η in a $D/M/2$.

ACKNOWLEDGMENT

This work is part of the IntellIoT project that received funding from the European Union’s Horizon 2020 research and innovation program under grant agreement No. 957218.

REFERENCES

- [1] S. Kavanagh, A. Luxton-Reilly, B. Wuensche, and B. Plimner, “A systematic review of Virtual Reality in education,” *Themes in Science and Technology Education*, vol. 10, no. 2, pp. 85–119, Dec. 2017.
- [2] D. Freeman, S. Reeve, A. Robinson, A. Ehlers, D. Clark, B. Spanlang, and M. Slater, “Virtual reality in the assessment, understanding, and treatment of mental health disorders,” *Psychological Medicine*, vol. 47, no. 14, pp. 2393–2400, Oct. 2017.
- [3] M. Farshid, J. Paschen, T. Eriksson, and J. Kietzmann, “Go boldly!: Explore augmented reality (AR), virtual reality (VR), and mixed reality (MR) for business,” *Business Horizons*, vol. 61, no. 5, pp. 657–663, Sep. 2018.
- [4] R. P. Singh, M. Javaid, R. Kataria, M. Tyagi, A. Haleem, and R. Suman, “Significant applications of virtual reality for COVID-19 pandemic,” *Diabetes & Metabolic Syndrome: Clinical Research & Reviews*, vol. 14, no. 4, pp. 661–664, Jul. 2020.

- [5] T. Chakraborti, S. Sreedharan, A. Kulkarni, and S. Kambhampati, "Projection-aware task planning and execution for human-in-the-loop operation of robots in a mixed-reality workspace," in *International Conference on Intelligent Robots and Systems (IROS)*. IEEE, Oct. 2018, pp. 4476–4482.
- [6] A. Bröring, V. Kulkarni, A. Zirkler, K. Fysarakis, S. Mayer, B. Soret, L. D. Nguyen, P. Popovski, S. Samarakoon, M. Bennis, J. Harri, M. Rooker, G. Fritz, A. Bucur, G. Spanoudakis, and S. Ionannidis, "IntellIoT: Intelligent, real-time, and trusted IoT environments with human-in-the-loop," *Submitted to European Conference on Networks and Communications*, 2021.
- [7] T. Braud, Z. Pengyuan, J. Kangasharju, and H. Pan, "Multipath computation offloading for mobile augmented reality," in *International Conference on Pervasive Computing and Communications (PerCom)*. IEEE, Mar. 2020.
- [8] M. Li, K. Arning, L. Vervier, M. Ziefle, and L. Kobbelt, "Influence of temporal delay and display update rate in an augmented reality application scenario," in *14th International Conference on Mobile and Ubiquitous Multimedia*. ACM, 2015, pp. 278–286.
- [9] J. Wu, B. Cheng, C. Yuen, N.-M. Cheung, and J. Chen, "Trading delay for distortion in one-way video communication over the internet," *IEEE Trans. on Circuits and Sys. for Video Tech.*, vol. 26, no. 4, pp. 711–723, 2016.
- [10] S. Kaul, R. Yates, and M. Gruteser, "Real-time status: How often should one update?" in *International Conference on Computer Communications (INFOCOM)*. IEEE, Mar. 2012, pp. 2731–2735.
- [11] M. Kazemi, S. Shirmohammadi, and K. H. Sadeghi, "A review of multiple description coding techniques for error-resilient video delivery," *Multimedia Systems*, vol. 20, no. 3, pp. 283–309, Jun. 2014.
- [12] C. Raiciu, S. Barre, C. Pluntke, A. Greenhalgh, D. Wischik, and M. Handley, "Improving datacenter performance and robustness with multipath TCP," *ACM SIGCOMM Computer Communication Review*, vol. 41, no. 4, pp. 266–277, Aug. 2011.
- [13] J. Rao and S. Vrzic, "Packet duplication for URLLC in 5G: Architectural enhancements and performance analysis," *IEEE Network*, vol. 32, no. 2, pp. 32–40, Apr. 2018.
- [14] F. Chiariotti, S. Kucera, A. Zanella, and H. Claussen, "Analysis and design of a latency control protocol for multi-path data delivery with pre-defined QoS guarantees," *IEEE/ACM Trans. on Net.*, vol. 27, no. 3, pp. 1165–1178, Jun. 2019.
- [15] S. Ferlin, S. Kucera, H. Claussen, and Ö. Alay, "MPTCP meets FEC: Supporting latency-sensitive applications over heterogeneous networks," *IEEE/ACM Transactions on Networking*, vol. 26, no. 5, pp. 2005–2018, Aug. 2018.
- [16] T. Mekonnen, P. Porambage, E. Harjula, and M. Ylianttila, "Energy consumption analysis of high quality multi-tier wireless multimedia sensor network," *IEEE Access*, vol. 5, pp. 15 848–15 858, Aug. 2017.
- [17] M. Z. Hasan, H. Al-Rizzo, and F. Al-Turjman, "A survey on multipath routing protocols for QoS assurances in real-time wireless multimedia sensor networks," *IEEE Communications Surveys & Tutorials*, vol. 19, no. 3, pp. 1424–1456, Jan. 2017.
- [18] X. Ge, L. Pan, Q. Li, G. Mao, and S. Tu, "Multipath cooperative communications networks for augmented and virtual reality transmission," *IEEE Transactions on Multimedia*, vol. 19, no. 10, pp. 2345–2358, Jul. 2017.
- [19] A. Ford, C. Raiciu, M. Handley, O. Bonaventure, and C. Paasch, "TCP extensions for multipath operation with multiple addresses," IETF, RFC 6824, Jan. 2013. [Online]. Available: <https://rfc-editor.org/rfc/rfc6824.txt>
- [20] E. Brosh, S. A. Baset, V. Misra, D. Rubenstein, and H. Schulzrinne, "The delay-friendliness of TCP for real-time traffic," *IEEE/ACM Transactions On Networking*, vol. 18, no. 5, pp. 1478–1491, Jun. 2010.
- [21] Y.-C. Chen, Y.-s. Lim, R. J. Gibbens, E. M. Nahum, R. Khalili, and D. Towsley, "A measurement-based study of Multipath TCP performance over wireless networks," in *SIGCOMM Internet Measurement Conf. (IMC)*. ACM, Oct. 2013, pp. 455–468.
- [22] P. Hurtig, K.-J. Grinnemo, A. Brunstrom, S. Ferlin, Ö. Alay, and N. Kuhn, "Low-latency scheduling in MPTCP," *IEEE/ACM Trans. on Net.*, vol. 27, no. 1, pp. 302–315, Dec. 2018.

- [23] R. Khalili, N. Gast, M. Popovic, and J.-Y. Le Boudec, “MPTCP is not Pareto-optimal: performance issues and a possible solution,” *IEEE/ACM Trans. on Net.*, vol. 21, no. 5, pp. 1651–1665, Oct. 2013.
- [24] F. Silva, M. A. Togou, and G.-M. Muntean, “AVIRA: Enhanced multipath for content-aware adaptive virtual reality,” in *International Wireless Communications and Mobile Computing (IWCMC)*. IEEE, Jun. 2020, pp. 917–922.
- [25] V. Singh, S. Ahsan, and J. Ott, “MP RTP: multipath considerations for real-time media,” in *4th Multimedia Systems Conference (MMSys)*. ACM, Feb. 2013, pp. 190–201.
- [26] T. D. Wallace and A. Shami, “Concurrent multipath transfer using SCTP: Modelling and congestion window management,” *IEEE Transactions on Mobile Computing*, vol. 13, no. 11, pp. 2510–2523, Feb. 2014.
- [27] O. C. Kwon, Y. Go, Y. Park, and H. Song, “MPMTP: Multipath multimedia transport protocol using systematic raptor codes over wireless networks,” *IEEE Transactions on Mobile Computing*, vol. 14, no. 9, pp. 1903–1916, Oct. 2014.
- [28] M. Polese, F. Chiariotti, E. Bonetto, F. Rigotto, A. Zanella, and M. Zorzi, “A survey on recent advances in transport layer protocols,” *IEEE Communication Surveys and Tutorials*, vol. 24, no. 4, pp. 3584–3608, Aug. 2019.
- [29] C. Kim and A. K. Agrawala, “Analysis of the fork-join queue,” *IEEE Transactions on Computers*, vol. 38, no. 2, pp. 250–255, Feb. 1989.
- [30] W. R. KhudaBukhsh, A. Rizk, A. Frömmgen, and H. Koepl, “Optimizing stochastic scheduling in fork-join queueing models: Bounds and applications,” in *Conference on Computer Communications (INFOCOM)*. IEEE, May 2017, pp. 1–9.
- [31] G. Joshi, E. Soljanin, and G. Wornell, “Efficient redundancy techniques for latency reduction in cloud systems,” *ACM Transactions on Modeling and Performance Evaluation of Computing Systems (TOMPECS)*, vol. 2, no. 2, pp. 1–30, Feb. 2017.
- [32] N. B. Shah, K. Lee, and K. Ramchandran, “When do redundant requests reduce latency?” *IEEE Transactions on Communications*, vol. 64, no. 2, pp. 715–722, Dec. 2015.
- [33] Y. Sun, C. E. Koksal, and N. Shroff, “On delay-optimal scheduling in queueing systems with replications,” *ArXiv*, vol. abs/1603.07322, Mar. 2016.
- [34] A. Rizk, F. Poloczek, and F. Ciucu, “Stochastic bounds in fork-join queueing systems under full and partial mapping,” *Queueing Systems*, vol. 83, no. 3, pp. 261–291, Aug. 2016.
- [35] M. Fidler and Y. Jiang, “Non-asymptotic delay bounds for (k, l) fork-join systems and multi-stage fork-join networks,” in *35th Annual International Conference on Computer Communications (INFOCOM)*. IEEE, Apr. 2016.
- [36] M. A. Abd-Elmagid, N. Pappas, and H. S. Dhillon, “On the role of age of information in the Internet of Things,” *IEEE Communications Magazine*, vol. 57, no. 12, pp. 72–77, Dec. 2019.
- [37] L. Huang and E. Modiano, “Optimizing age-of-information in a multi-class queueing system,” in *International Symposium on Information Theory (ISIT)*. IEEE, Jun. 2015, pp. 1681–1685.
- [38] Y. Inoue, H. Masuyama, T. Takine, and T. Tanaka, “A general formula for the stationary distribution of the Age of Information and its application to single-server queues,” *IEEE Transactions on Information Theory*, vol. 65, no. 12, pp. 8305–8324, Dec. 2019.
- [39] A. Kosta, N. Pappas, V. Angelakis *et al.*, “Age of information: A new concept, metric, and tool,” *Foundations and Trends in Networking*, vol. 12, no. 3, pp. 162–259, Nov. 2017.
- [40] R. D. Yates, “The age of information in networks: Moments, distributions, and sampling,” *IEEE Transactions on Information Theory*, vol. 66, no. 9, pp. 5712–5728, May 2020.
- [41] X. Chen, K. Gatsis, H. Hassani, and S. S. Bidokhti, “Age of information in random access channels,” in *International Symposium on Information Theory (ISIT)*. IEEE, Jun. 2020, pp. 1770–1775.
- [42] A. Munari, “Modern random access: an age of information perspective on Irregular Repetition Slotted ALOHA,” *IEEE Transactions on Communications*, Feb. 2021.

- [43] J. Li, Y. Zhou, and H. Chen, “Age of information for multicast transmission with fixed and random deadlines in IoT systems,” *IEEE Internet of Things Journal*, vol. 7, no. 9, pp. 8178–8191, Mar. 2020.
- [44] F. Chiariotti, O. Vikhrova, B. Soret, and P. Popovski, “Peak age of information distribution for edge computing with wireless links,” *IEEE Transactions on Communications*, Jan. 2021.
- [45] N. Akar, O. Doğan, and E. U. Atay, “Finding the exact distribution of (Peak) Age of Information for queues of PH/PH/1/1 and M/PH/1/2 type,” *IEEE Transactions on Communications*, vol. 68, no. 9, pp. 5661–5672, Jun. 2020.
- [46] B. Buyukates and S. Ulukus, “Timely distributed computation with stragglers,” *IEEE Transactions on Communications*, vol. 68, no. 9, pp. 5273–5282, Jun. 2020.
- [47] R. Talak and E. H. Modiano, “Age-delay tradeoffs in queueing systems,” *IEEE Transactions on Information Theory*, vol. 67, no. 3, pp. 1743–1758, Mar. 2021.
- [48] A. K. Erlang, “Løsning af nogle problemer fra sandsynlighedsregningen af betydning for de automatiske telefoncentraler,” *Elektroteknikerens*, vol. 13, pp. 5–13, Jan. 1917.
- [49] D. Pinotsi and M. A. Zazanis, “Synchronized queues with deterministic arrivals,” *Operations Research Letters*, vol. 33, no. 6, pp. 560–566, Nov. 2005.
- [50] F. Baccelli and P. Brémaud, *Palm probabilities and stationary queues*, ser. Lecture Notes in Statistics. Springer Verlag, Dec. 2012, vol. 41.